HHS Public Access

Author manuscript

Colloids Surf B Biointerfaces. Author manuscript; available in PMC 2020 August 01.

Published in final edited form as:

Colloids Surf B Biointerfaces. 2019 August 01; 180: 371–375. doi:10.1016/j.colsurfb.2019.05.001.

Engineering Functional Hydrogel Microparticle Interfaces by Controlled Oxygen-Inhibited Photopolymerization

Daniel Debroy, **Katie Dongmei Li-Oakey***, and **John Oakey***

Department of Chemical Engineering, University of Wyoming, Laramie, WY 82071

Abstract

Functional poly(ethylene glycol) diacrylate (PEGDA) hydrogel microparticles for the detection of bioactive macromolecules were fabricated *via* oxygen-inhibited photopolymerization in a droplet microfluidic device. Hydrogel network functionalization and architecture were characterized using a biotin-avidin binding assay, which revealed radial network inhomogeneities dependent on exposure conditions. Empirical results were corroborated using a reaction-diffusion model, describing the effects of exposure intensity on the spatial photopolymerization kinetics and resulting polymeric mesh network. The combination of finely controlled exposure conditions and predictive simulations enables the generation of tailored particles with microengineered interfaces and gradients in crosslinking density, which dictate solute diffusivity and elasticity, augmenting the utility of this approach in engineering multifunctional, size-excluding hydrogel particles for multiplexed biomolecular sensing.

Graphical Abstract:

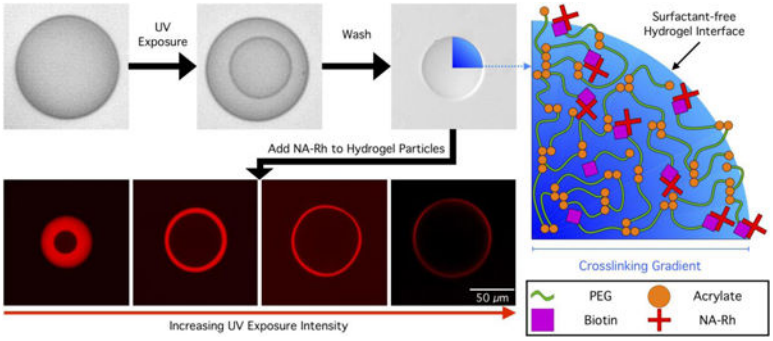

Introduction

Synthetic, photopolymerized hydrogels are versatile and widely used biomaterials that consist of highly crosslinked, water-swollen, sample-spanning polymer networks.[1] Techniques to tailor hydrogel network properties are commonly used to control the

*To whom correspondence should be addressed., joakey@uwyo.edu, dli1@uwyo.edu.

conjugation, steric encapsulation, and release of bioactive macromolecules. Hydrogels composed of poly(ethylene glycol) diacrylate (PEGDA) have attracted particular and widespread interest due to their fabrication versatility and high degree of tunability.[2] Diacrylated PEG-containing block copolymers have been used to form hydrogels with dynamic network properties enabling them to be used for a diversity of applications in various microenvironments.[3,4] Photoinitiated polymerization lends exquisite spatial and temporal control over polymerization kinetics[5] as well as the ability to lithographically pattern PEGDA hydrogel structures with dimensions on the micrometer scale. Microscale hydrogels have been used as drug delivery vehicles,[6] tissue scaffolds,[7] biosensors,[8] and diagnostic platforms.[9]

Various applications for hydrogels benefit from the direct conjugation of functional moieties to the hydrogel network in order to impart heterogeneous spatial properties and function.[10,11] Biosensing applications particularly rely on the copolymerization of proteins and enzymes in the hydrogel network for detection and quantification of specific analytes.[12–14] Hydrogel microparticle-based biosensing platforms possess many advantages over benchtop techniques, such as low cost, greater detection sensitivity, small sample consumption, multiplexing, and the ability to perform on-site analysis.[15–18] Hydrogel microparticles have been produced *via* a variety of methods, including suspension, emulsion, and precipitation polymerization and photolithographic techniques.[19] Stop flow lithography (SFL) has many advantages over batch techniques due to its fine control over particle size, shape, and network properties and has been used to fabricate bar-coded hydrogel microparticles for multiplexed protein and nucleic acid detection and quantification.[20,21] The introduction of mesh size gradients in hydrogel microparticles generated using SFL further increases detection specificity by incorporating molecular size exclusion capabilities, enabling the size-selective sieving of molecules such as mRNA.[22,23] Despite its versatility, SFL can only generate particles with internal mesh size gradients via macromer molecular weight gradients formed by laminar flow lithography[21] or gradient generators,[24] or through the use of porogens.[22] SFL is also an inherently low throughput (<5 Hz) production method.[21] To address these challenges, here we report a high-throughput technique that enables the continuous generation of hydrogel particles with complex and tunable network properties without the need for porogens or graded material precursors.

Droplet microfluidics, a technique used to produce emulsion droplets by merging two coflowing immiscible fluid phases, has emerged as a versatile and high-throughput alternative, allowing the continuous production of monodisperse microparticles[25] that can be easily functionalized.[26] Polydimethylsiloxane (PDMS) is commonly used to construct droplet microfluidic devices, because it is inexpensive, hydrophobic, and transparent, which facilitates imaging and coupling of a UV light source to photopolymerize flowing droplets *in situ*.[27] The high gas permeability of PDMS, combined with the high oxygen solubility of fluorocarbon carrier oils commonly used for droplet formation, renders droplets polymerized in PDMS-based microchannels susceptible to oxygen inhibition.[28] This phenomenon refers to the quenching of primary initiating or propagating radicals by oxygen to form peroxyl radicals. Since peroxyl radicals do not initiate acrylate double bond conversion, radical chain polymerization cannot proceed until dissolved oxygen is consumed almost completely.[29,30] The competition between the diffusion and consumption of oxygen is evident in droplets due

to the constant replenishment of oxygen over the short diffusion length scales across the oil-aqueous interface to the aqueous core. As a consequence, exposed droplets possess a polymerized core and unpolymerized shell, with the thickness of shell being determined by the diffusion and reaction of oxygen. While generally deleterious to many biological applications,[31] oxygen inhibition has been previously exploited to produce hydrogel particles in droplet templates with precise size control.[32] Additionally, a predictive reaction-diffusion model was developed to fully describe particle-to-droplet diameter ratio as a function of processing parameters during oxygen-inhibited particle photopolymerization in emulsion droplets.

Controlled oxygen-inhibited droplet photopolymerization presents a unique platform in which immunofunctional hydrogel particles with precisely microengineered interfaces can be produced in a high-throughput fashion. Further, rigorous control over exposure conditions enables exquisite manipulation of the internal network architecture of these particles without the need for porogens. This technique is demonstrated by fabricating particles with biotin-decorated hydrogel networks which are subsequently incubated within a fluoro-neutravidin solution. Specific binding of the tagged ligand reveals the availability of copolymerized functional groups at the particle surface and neutravidin's (NA) accessibility to the particle interior. Additionally, experimental results are corroborated with a reaction-diffusion model that describes the effect of photopolymerization kinetics on local hydrogel network architecture. The integrated approach of combining experimental results and model prediction enables the fabrication of particles with a range of controllable spatial gradients in their degree of crosslinking. For example, weakly crosslinked particles allow NA to diffuse across their entire radius, while the highly crosslinked particles are completely impenetrable to NA. As crosslinking increases, biotin accessibility becomes sterically constrained entirely by the polymeric mesh network. These bounding cases highlight the tractability of this fabrication approach and illustrate the importance of considering photopolymerization conditions when microfabricating particles for biosensing applications. Particles fabricated by this platform can be designed with gradients in crosslinking density, diffusive conductivity, and elasticity, highlighting the utility of this approach in engineering multifunctional, size-excluding hydrogel particles for biomolecular sensing.

Experimental Section

Hydrogel forming solution preparation: A solution composed of 0.38 M PEGDA 700, 17 mM Lithium phenyl-2,4.6-trimethylbenzoylphosphinate (LAP), and 2.1 mM Acryl-PEG-Biotin (2000 Da) in a phosphate buffered saline (PBS, GenClone) was used as the aqueous phase, and a fluorocarbon oil (Novec 7500 + 2% Picosurf 1, Dolomite) was used as the oil phase for the microfluidic droplet process.

Neutravidin-Rhodamine preparation: Neutravidin (Na) was conjugated to NHS-Rhodamine (NHS-Rh) according to the protocol provided by Thermo Scientific, and diluted to a concentration of 0.43 mg/ml.

Microfluidic device preparation and operation: Flow focusing PDMS microfluidic devices were prepared using standard soft lithography techniques. [33] Briefly, a two layer

photoresist pattern was fabricated by two sequential UV exposure steps with two different photomasks to obtain different channel depths for each device section: 30 μm for the droplet pinch-off section, and 110 μm for the downstream photopolymerization section.

Liquid flow was delivered to and controlled within the device using a series of syringe pumps (neMESYS), flowing at 20 μl/hr for the aqueous phase, 40 μl/hr for the continuous oil phase, and 140 μl/hr for the downstream oil phase (see Figure S1). At these flow rates, droplets with diameters of 100 μm were formed at a rate of 11 Hz, a higher frequency than similar particle generating techniques,[21] and exposed for 708 ± 15 ms. Droplets were photopolymerized using a white light LED source with a DAPI filter (350–400 nm) and a 10x objective (Olympus UPlanFLN 10X/0.30Ph1). After collecting particles for 15 minutes, 1 ml of deionized water was added, and the mixture was vortexed for 30s to wash away the unpolymerized shell, after which the particles were separated from the oil and most of the water using a 5 μm centrifuge filter (1350 rpm for 5 min), and recovered particles were resuspended in 400 μl of PBS. 30 μl aliquots of the particle mixture were combined with 7.5 μl of the Na-Rh solution and mixed for two days, after which the particles were washed and resuspended in 100 μl PBS, incubated for 2 days to allow unincorporated Na-Rh to diffuse out, and imaged.

For fluorescent imaging, a 20x objective was used in combination with a white light source filtered with a Texas Red filter cube (Ex: 535–580 nm, Em: 590–670 nm). A high-resolution camera (QIClick, QImaging) was used to collect images of 30 particles for each exposure intensity, using an exposure time of 100 ms. Confocal images were acquired using an Olympus IX-81 microscope equipped with a Yokogawa spinning disk (CSU X1) and a scientific complementary metal-oxide semiconductor (sCMOS) camera (Orca-FLASH 4.0, Hammatsu). Two objectives (20x and 60x) were used to acquire confocal images. ImageJ was used to obtain an averaged radial profile of the fluorescent intensity for each particle and, after normalizing each data set, the average profile was calculated. The best-fit extent of conversion threshold value was established by calculating the coefficient of determination (R^2) between the experimental Na-Rh penetration depth and the predicted penetration depth at a given extent of conversion value. This statistical analysis is presented in Figure S2, where the maximum R^2 value corresponded to 38% extent of conversion.

Results and Discussion

Photopolymerizable emulsions were formed using a flow-focusing PDMS microfluidic device and polymerized in situ. Figure 1 is a schematic representation of the copolymerization of acryl-PEG-biotin with PEGDA to form a hydrogel microparticle via photopolymerization in a microfluidic device under ambient conditions. Continuous generation of hydrogel droplets within microfluidic devices enables facile and reproducible control over the composition of each droplet as it is being formed, presenting a unique advantage over batch polymerization processes. Upon exposure to UV light, a polymerized hydrogel core, surrounded by an unpolymerized shell is formed as a consequence of oxygen inhibition, as previously described.[28,32] The thickness of this shell and, consequently, the size of the polymerized core can be easily tuned by adjusting the droplet composition and exposure intensity. The unpolymerized shell, along with surfactant retained at the droplet

interface, can be removed via sonication and centrifugation to produce particles with surface properties distinct from that of the parent droplets. The ease of surfactant removal presents yet another advantage of oxygen-inhibited photopolymerization relative to fully-polymerized particles produced in an oxygen-depleted environment, in which the surfactant molecules remain entangled in the hydrogel network at the interface, requiring a second surfactant to re-suspend the particles in an aqueous solution. Surfactant-coated hydrogel interfaces can modify surface interactions and even make the particle surface and functional groups tethered to it inaccessible.

To visualize and quantify the concentration and availability of biotin groups copolymerized in the hydrogel network during the photopolymerization process, particles were incubated within a solution containing Neutravidin-Rhodamine (NA-Rh), which diffused into the hydrogel and bound specifically to biotin. Subsequently hydrogel particles were thoroughly washed and re-suspended in buffer. The strong avidin-biotin affinity retained NA-Rh within the particles, ensuring that fluorescence observed after rinsing was the result of NA-Rh bound to the biotin in the hydrogel network. Fluorescent imaging of particles (Figure 1B) revealed NA-Rh was distributed inhomogeneously throughout the hydrogel network, suggesting that either the hydrogel network or the availability or activity of biotin displayed spatial variation. Imaging the fluorescent intensity distribution within particles while still immersed in the NA-Rh solution show that the particle core is inaccessible to NA, even after long incubation times. After particle washing, the gradient in fluorescent intensity became apparent, revealing that bound NA was retained in a radially varying manner. It has been previously reported that oxidized biotin does not lose affinity or binding capacity to avidin groups.[34] As Acryl-PEG-Biotin is incorporated into the hydrogel network in a statistical proportion to PEGDA,[35] it follows that the observed NA-Rh intensity traces the crosslinking density of the hydrogel network.

To quantitatively explore this phenomenon, four discrete exposure intensities were used to photopolymerize droplets, while holding all other processing parameters, such as droplet composition and exposure time, constant. Increasing exposure intensity accelerates the rate of photoinitiator radical production. In addition to reducing the unpolymerized shell thickness, increasing UV intensity should affect the rate of macromer conversion and crosslinking. Particles would therefore be generated with crosslinking maxima at the center, crosslinking minima at their surface, and radial crosslinking density profiles that vary nonlinearly with transient oxygen concentration during photopolymerization. As seen in Figure 2B, particles produced with varying exposure intensity indeed differ not only in size, but also in the final distribution of NA-Rh throughout the particle. Clearly, the radial crosslinking density gradient within the hydrogel network allowed NA molecules, globular proteins with a molecular weight of roughly 60k Da, to penetrate to a given radial position at which point the hydrogel mesh size becomes too constricted to allow NA diffusion. This penetration length can be visualized as a fluorescent shell surrounding a dark spherical core. This has been observed previously in hydrogel particles for nucleic acid hybridization assays,[16] but the photopolymerization kinetics and their effect on hydrogel network properties were not described.

Radially-averaged NA-Rh fluorescent intensity profiles corresponding to each UV exposure intensity used in Figure 2 are summarized in Figure 3. Two distinct regions can be defined in the hydrogel network using the radial position of the maximum florescence intensity of this profile, r_{max} (Figure 3, indicated by a vertical dotted line). When $r > r_{max}$, the fluorescent intensity corresponds to the availability of biotin copolymerized into the hydrogel network, and therefore can be used as a descriptor of the local crosslinking density. Since oxygen-inhibited photopolymerization within an emulsion droplet generates a radial conversion gradient, a biotin concentration gradient copolymerized with the crosslinked network decays sharply near the particle surface. For $r < r_{max}$, the fluorescent intensity is no longer a function of the copolymerized biotin concentration and decreases rapidly toward the more homogeneously crosslinked core where very little or no detectable fluorescence can be observed. The exclusion of NA-Rh from the particle core is a consequence of increased crosslinking density and therefore decreased mesh size, which restricts the diffusion of NA-Rh.

To elucidate the relationship between oxygen inhibited photopolymerization kinetics and network architecture, a transient reaction-diffusion model was developed to fully describe hydrogel formation within a single droplet. A full description of this model can be found in the Supplementary Information. The model enables predictions of radial extent of conversion, the amount of macromer locally incorporated into the hydrogel network, which is directly related to the degree of crosslinking for bifunctional macromer units. The extent of macromer conversion, and thus crosslinking density, consequently dictate the hydrogel's network properties. It has been previously shown that an increase in the extent of conversion results in diminished permeability and diffusivity of solutes in PEGDA hydrogels.[36] Figure 3 summarizes the observed correlation between model prediction of extent of conversion and experimental intensity results. Both data sets are functions of the droplet/particle radius. Previous reports suggest that gelation can be observed above a minimum threshold conversion of 2%.[37] Previously, we validated the accuracy of the reaction-diffusion model in predicting particle size from a particular droplet and given processing parameters.[32] As shown in Figure 3, the particle size corresponds to the predicted 2% extent of conversion value. It is instructive that for the four different exposure intensity plots all four maxima lines intersected the respective predicted extent of conversion curves at the same value of 38%. The consistent matching of the NA penetration cutoff to a predicted 38% extent of conversion confirms that the hydrogel network surpasses a threshold crosslinking density at which NA-Rh diffusion is restricted. This is further corroborated by Figure 4, which summarizes model predicted radial positions at which the extent of conversion was 38% (dotted line). These predictions accurately describe empirical observations for the observed NA penetration depth.

Developing an understanding of the coupled oxygen and macromer conversion gradients is important in the design of hydrogels for applications other than biosensing, such as drug delivery, in which water content, gel swelling, hydrolytic degradation rate, modulus, stiffness, and hydrophobicity are all affected by the crosslinking density.[38] Additionally, fine-tuned control of oxygen-inhibited photopolymerization presents a unique opportunity to optimize the availability of functional groups within and at the surface of hydrogel particles. Beyond a threshold conversion, copolymerized functional groups will strictly be accessible

at the interface, since the hydrogel network mesh will be too highly crosslinked to allow molecular diffusion into the network. Since the threshold conversion scales inversely with solute size, carefully decreasing the conversion will enable diffusion into the network with well-controlled penetration lengths. For biosensing applications, dense networks that are highly crosslinked at the particle surface suppress sensitivity by presenting fewer accessible functional groups. In contrast, lower UV intensity produced open network architectures with well-defined gradients, which are useful for enhancing bioassay detection sensitivity of biomolecules with different sizes.[22]

Other processing variables, such as exposure time, monomer concentration, and monomer chain length, will also impact the gradient formation process and final network architecture of hydrogel microparticles in a predictable manner. For example, decreasing monomer concentration or increasing monomer molecular weight would result in a looser hydrogel network, facilitating the diffusion of larger molecules into the particle. Well-known models are able to predict solute diffusion based solely on solution stoichiometry but disregard extent of conversion effects.[39] Likewise, PEGDA hydrogel network architecture and its dependent properties are typically reported in terms of monomer concentration and molecular weight, disregarding the effects of exposure conditions.[40,41] A comprehensive model that incorporates these effects will be instructive in designing particles with specific network properties for a diverse number of applications, including tuning particle degradation rates, release profiles of encapsulated components, and interaction with microenvironments by modulating particle elasticity. The careful control of hydrogel crosslinking density gradients can also be exploited to generate unique mechanical properties for tissue engineering. While results here were collected using particles with a size range of 60–100 μm, they may be extrapolated to larger or smaller particles produced using oxygen-inhibited photopolymerization. Using this platform to develop a deeper understanding of hydrogel photopolymerization at oxygen-rich interfaces is instructive in applications beyond particle generation, such as hydrogel tissue scaffold engineering and stereolithography-based 3D printing.

Conclusion

We report a hydrogel microparticle fabrication platform that enables the generation of radial crosslinking density gradients by exploiting oxygen-inhibited photopolymerization in a microfluidic device. This platform overcomes the limitations of previously reported techniques, such as SFL, by facilitating the continuous, high-throughput generation of custom hydrogel particles without the need for porogens or graded material precursors.[21–23] The application of these particles as macromolecular biosensors by incorporating biofunctional molecules was demonstrated using a model biotin-avidin assay, which revealed network architecture dependence on local gelation kinetics and operating parameters. The generation of radial crosslinking density gradients was empirically observed as a diffusive limitation of NA-Rh into the particle past a critical penetration depth, which was dependent on UV exposure intensity. Experimental observations were corroborated with a reaction-diffusion model that predicted a constant threshold conversion of 38%, which matched the penetration depth for different exposure intensities. The accurate predictive capabilities provided by this reaction-diffusion model can be applied to easily design

hydrogel particles with custom network architectures based on photopolymerization conditions. While this work focused on the detection of mobile species following their diffusion into the particle, these particles can also be utilized in drug delivery and tissue engineering applications, where the careful modulation of particle degradation and molecular release is critical.

Supplementary Material

Refer to Web version on PubMed Central for supplementary material.

Acknowledgements

This work was funded by the NSF Faculty CAREER Program to JO (BBBE 1254608) and by the NIH-funded Wyoming IDeA Networks of Biomedical Research Excellence program to DL (P20GM103432). We also thank Professor Jesse Gatlin and Taylor Sulerud for their generous assistance with confocal imaging.

References

(1). Liu AL; García AJ Methods for Generating Hydrogel Particles for Protein Delivery. Annals of Biomedical Engineering 2016, 44 (6), 1946–1958. [PubMed: 27160672]

(2). Hwang DK; Oakey J; Toner M; Arthur JA; Anseth KS; Lee S; Zeiger A; Van Vliet KJ; Doyle PS Stop-Flow Lithography for the Production of Shape-Evolving Degradable Microgel Particles. J. Am. Chem. Soc 2009, 131 (12), 4499–4504. [PubMed: 19215127]

(3). DeForest CA; Polizzotti BD; Anseth KS Sequential Click Reactions for Synthesizing and Patterning Three-Dimensional Cell Microenvironments. Nature Materials 2009, 8 (8), 659–664. [PubMed: 19543279]

(4). Kloxin AM; Tibbitt MW; Anseth KS Synthesis of Photodegradable Hydrogels as Dynamically Tunable Cell Culture Platforms. Nature Protocols 2010, 5 (12), 1867–1887. [PubMed: 21127482]

(5). Zhu J Bioactive Modification of Poly(Ethylene Glycol) Hydrogels for Tissue Engineering. Biomaterials 2010, 31 (17), 4639–4656. [PubMed: 20303169]

(6). Ahmad M; Rai SM; Mahmood A Hydrogel Microparticles as an Emerging Tool in Pharmaceutical Field: a Review. Adv. Polym. Technol 2015, 35 (2), 121–128.

(7). Burdick JA; Anseth KS Photoencapsulation of Osteoblasts in Injectable RGD-Modified PEG Hydrogels for Bone Tissue Engineering. Biomaterials 2002, No. 23, 4315–4323. [PubMed: 12219821]

(8). Buenger D; Topuz F; Groll J Hydrogels in Sensing Applications. Progress in Polymer Science 2012, 37 (12), 1678–1719.

(9). Lee AG; Arena CP; Beebe DJ; Palecek SP Development of Macroporous Poly(Ethylene Glycol) Hydrogel Arrays Within Microfluidic Channels. Biomacromolecules 2010, 11 (12), 3316–3324. [PubMed: 21028794]

(10). Sakhalkar HS Enhanced Adhesion of Ligand-Conjugated Biodegradable Particles to Colitic Venules. The FASEB Journal 2005, 1–19. [PubMed: 15629889]

(11). Burdick JA; Khademhosseini A; Langer R Fabrication of Gradient Hydrogels Using a Microfluidics/Photopolymerization Process. Langmuir 2004, 20 (13), 5153–5156. [PubMed: 15986641]

(12). Yadavalli VK; Koh W-G; Lazur GJ; Pishko MV Microfabricated Protein-Containing Poly(Ethylene Glycol) Hydrogel Arrays for Biosensing. Sensors and Actuators B: Chemical 2004, 97 (2–3), 290–297.

(13). Rehman FN; Audeh M; Abrams ES; Hammond PW; Kenney M; Boles TC Immobilization of Acrylamide-Modified Oligonucleotides by Co-Polymerization. Nucleic Acids Res 1999, 27 (2), 649–655. [PubMed: 9862993]

(14). Kenney M; Ray S; Boles TC Mutation Typing Using Electrophoresis and Gel-Immobilized Acrydite. BioTechniques 1998, 25 (3), 516–521. [PubMed: 9762449]

(15). Lee Y; Choi D; Koh W-G; Kim B Poly(Ethylene Glycol) Hydrogel Microparticles Containing Enzyme-Fluorophore Conjugates for the Detection of Organophosphorus Compounds. Sensors and Actuators B: Chemical 2009, 137 (1), 209–214.

(16). Lewis CL; Choi C-H; Lin Y; Lee C-S; Yi H Fabrication of Uniform DNA-Conjugated Hydrogel Microparticles via Replica Molding for Facile Nucleic Acid Hybridization Assays. Anal. Chem 2010, 82 (13), 5851–5858. [PubMed: 20527819]

(17). Le Goff GC; Srinivas RL; Hill WA; Doyle PS Hydrogel Microparticles for Biosensing. European Polymer Journal 2015, 72 (C), 386–412. [PubMed: 26594056]

(18). Pregibon D; Toner M; Doyle P Multifunctional Encoded Particles for High-Throughput Biomolecule Analysis. Science 2007, 315, 1393–1396. [PubMed: 17347435]

(19). Helgeson ME; Chapin SC; Doyle PS Hydrogel Microparticles From Lithographic Processes: Novel Materials for Fundamental and Applied Colloid Science. Current Opinion in Colloid & Interface Science 2011, 16 (2), 106–117. [PubMed: 21516212]

(20). Appleyard DC; Chapin SC; Srinivas RL; Doyle PS Bar-Coded Hydrogel Microparticles for Protein Detection: Synthesis, Assay and Scanning. Nature Protocols 2011, 6 (11), 1761–1774. [PubMed: 22015846]

(21). Bong KW; Chapin SC; Doyle PS Magnetic Barcoded Hydrogel Microparticles for Multiplexed Detection. Langmuir 2010, 26 (11), 8008–8014. [PubMed: 20178351]

(22). Choi NW; Kim J; Chapin SC; Duong T; Donohue E; Pandey P; Broom W; Hill WA; Doyle PS Multiplexed Detection of mRNA Using Porosity-Tuned Hydrogel Microparticles. Anal. Chem 2012, 84 (21), 9370–9378. [PubMed: 23020189]

(23). Luchini A; Geho DH; Bishop B; Tran D; Xia C; Dufour RL; Jones CD; Espina V; Patanarut A; Zhou W; Ross MM; Tessitore A; Petricoin EF; Liotta LA Smart Hydrogel Particles: Biomarker Harvesting: One-Step Affinity Purification, Size Exclusion, and Protection Against Degradation. Nano Lett 2008, 8 (1), 350–361. [PubMed: 18076201]

(24). Mahadik BP; Wheeler TD; Skertich LJ; Kenis PJA; Harley BAC Microfluidic Generation of Gradient Hydrogels to Modulate Hematopoietic Stem Cell Culture Environment. Adv. Healthcare Mater 2013, 3 (3), 449–458.

(25). Teh S-Y; Lin R; Hung L-H; Lee AP Droplet Microfluidics. Lab Chip 2008, 8 (2), 198–23. [PubMed: 18231657]

(26). Kim JH; Jeon TY; Choi TM; Shim TS; Kim S-H; Yang S-M Droplet Microfluidics for Producing Functional Microparticles. Langmuir 2014, 30 (6), 1473–1488. [PubMed: 24143936]

(27). Dang T-D; Kim YH; Kim HG; Kim GM Preparation of Monodisperse PEG Hydrogel Microparticles Using a Microfluidic Flow-Focusing Device. Journal of Industrial and Engineering Chemistry 2012, 18 (4), 1308–1313.

(28). Krutkramelis K; Xia B; Oakey J Monodisperse Polyethylene Glycol Diacrylate Hydrogel Microsphere Formation by Oxygen-Controlled Photopolymerization in a Microfluidic Device. Lab Chip 2016, 16 (8), 1457–1465. [PubMed: 26987384]

(29). Decker C; Jenkins AD Kinetic Approach of O2 Inhibition in Ultraviolet- and Laser-Induced Polymerizations. Macromolecules 1985, 1241–1244.

(30). Ligon SC; Husár B; Wutzel H; Holman R; Liska R Strategies to Reduce Oxygen Inhibition in Photoinduced Polymerization. Chem. Rev 2014, 114 (1), 557–589. [PubMed: 24083614]

(31). Xia B; Jiang Z; Debroy D; Li D; Oakey J Cytocompatible Cell Encapsulation via Hydrogel Photopolymerization in Microfluidic Emulsion Droplets. Biomicrofluidics 2017, 11 (4), 044102–044111. [PubMed: 28794813]

(32). Debroy D; Oakey J; Li D Interfacially-Mediated Oxygen Inhibition for Precise and Continuous Poly(Ethylene Glycol) Diacrylate (PEGDA) Particle Fabrication. Journal of Colloid And Interface Science 2018, 510, 334–344. [PubMed: 28961432]

(33). Xia Y; Whitesides GM Soft Lithography. Annu. Rev. Mater. Sci 1998, 153–185.

(34). Melville D; Genghof D; Lee J Biological Properties of Biotin D- and L- Sulfoxides. J. Biol. Chem 1954, No. 208, 503–512. [PubMed: 13174560]

(35). Beamish JA; Zhu J; Kottke-Marchant K; Marchant RE The Effects of Monoacrylated Poly(Ethylene Glycol) on the Properties of Poly(Ethylene Glycol) Diacrylate Hydrogels Used for Tissue Engineering. J. Biomed. Mater. Res 2009, 9999A, NA–NA.

(36). Anseth KS; Metters AT; Bryant SJ; Martens PJ; Elisseeff JH; Bowman CN In Situ Forming Degradable Networks and Their Application in Tissue Engineering and Drug Delivery. Journal of Controlled Release 2002, 78, 199–209. [PubMed: 11772461]

(37). Andrzejewska E Photopolymerization Kinetics of Multifunctional Monomers. Progress in Polymer Science 2001, 26 (4), 605–665.

(38). Lin C-C; Anseth KS PEG Hydrogels for the Controlled Release of Biomolecules in Regenerative Medicine. Pharm Res 2008, 26 (3), 631–643. [PubMed: 19089601]

(39). Lustig S; Peppas NA Solute Diffusion in Swollen Membranes. IX. Scaling Laws for Solute Diffusion in Gels. Journal of Applied Polymer Science 1988, 735–747.

(40). Hagel V; Haraszti T; Boehm H Diffusion and Interaction in PEG-DA Hydrogels. Biointerphases 2013, 8 (36), 1–9. [PubMed: 24706114]

(41). Cruise G; Scharp D; Hubbell J Characterization of Permeability and Network Structure of Interfacially Photopolymerized Poly(Ethylene Glycol) Diacrylate Hydrogels. Biomaterials 1998, No. 19, 1287–1294. [PubMed: 9720892]

Highlights:

- PEG hydrogel particles with complex architecture are produced from droplet templates
- Particle interfaces can be engineered with predicted elasticity and diffusivity
- Oxygen inhibited acrylate conversion gives rise to variations in crosslinking density
- Crosslinking density gradients are formed from competing reaction diffusion rates
- A quantitative model validates empirical observation and provides predictive design

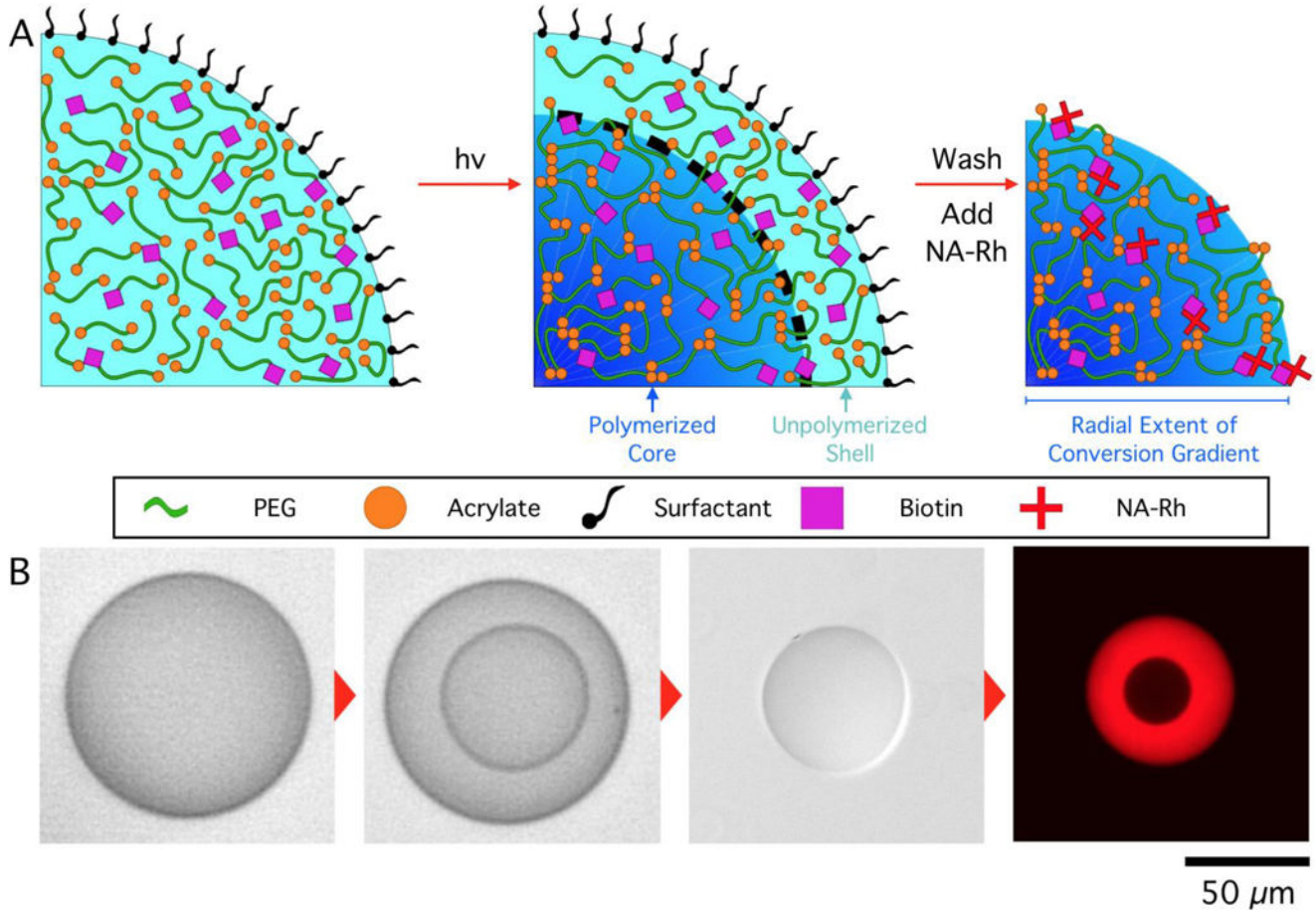

Figure 1.

Oxygen-inhibited photopolymerization of droplets containing Acryl-PEG-biotin produces functional hydrogels with surfactant-free surfaces. A. Schematic illustration of hydrogel microparticle fabrication via oxygen-inhibited photopolymerization. B. Micrographs illustrating the process described in A, with NA-Rh fluorescence imaging showing the presence of a radial crosslinking density gradient in the hydrogel network. Droplet content: 30 wt% PEGDA 700, 0.5 wt% LAP, 0.5 wt% Acryl-PEG-Biotin, exposed for 700 ms, 350 μW/cm^2.

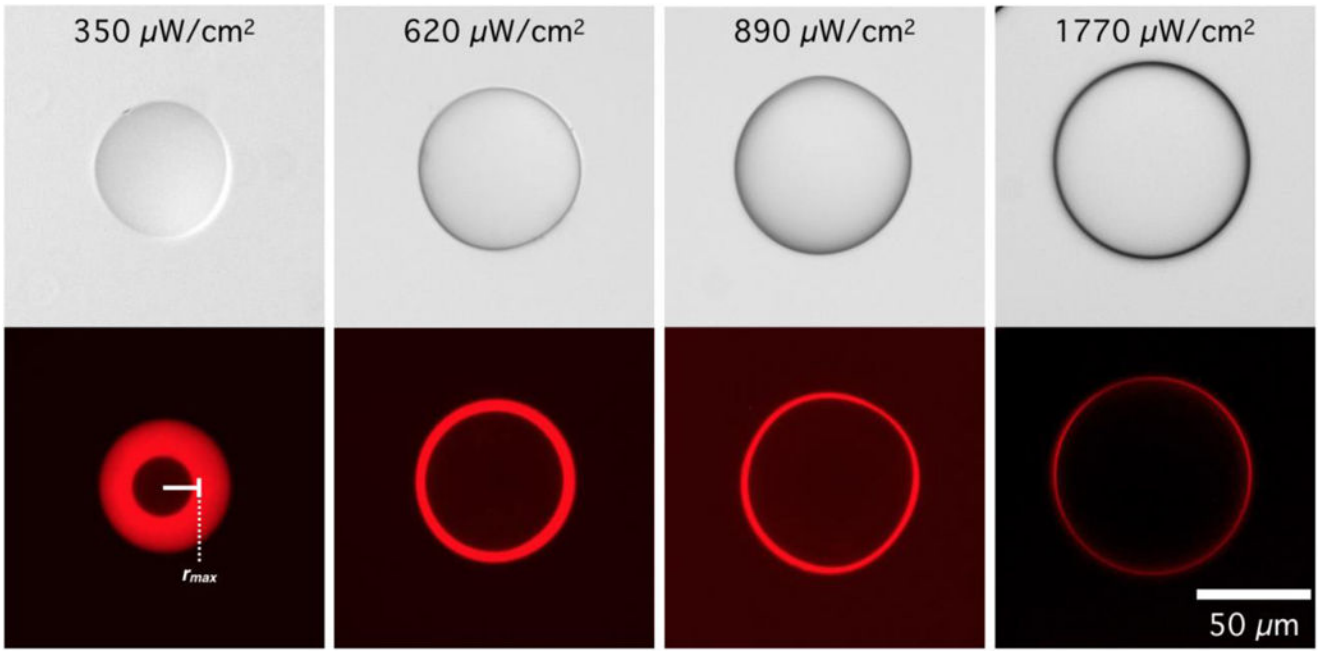

Figure 2.

A Biotin/Neutravidin-Rhodamine (NA-Rh) assay reveals that Neutravidin (NA) penetration is limited to a radial distance that is dictated by photopolymerization conditions. Elucidating the governing reaction-diffusion behavior allows the network architecture to be defined, dictating local hydrogel mechanical properties and biomolecular diffusion for applications such as drug release or bioassays. r_{max}: radial position of the maximum florescence intensity.

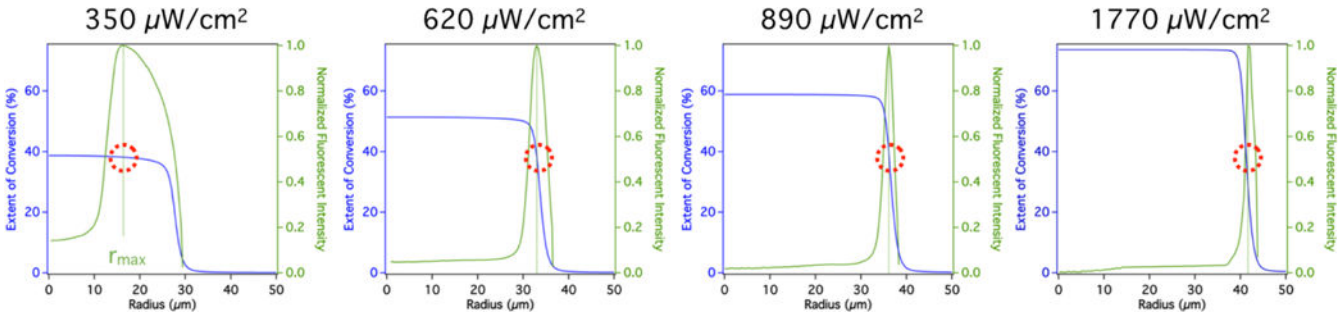

Figure 3.

Experimental fluorescent intensity (green) and reaction-diffusion model prediction of extent of conversion (blue) illustrate that the penetration of fluorescently tagged Neutravidin (NA) into the hydrogel particle is the consequence of constrained network architecture at increasing conversion. Above a threshold extent of conversion, the hydrogel mesh can no longer accommodate the diffusion of Neutravidin. 38% represents this threshold conversion value, while 2% is the extent required to achieve gelation.

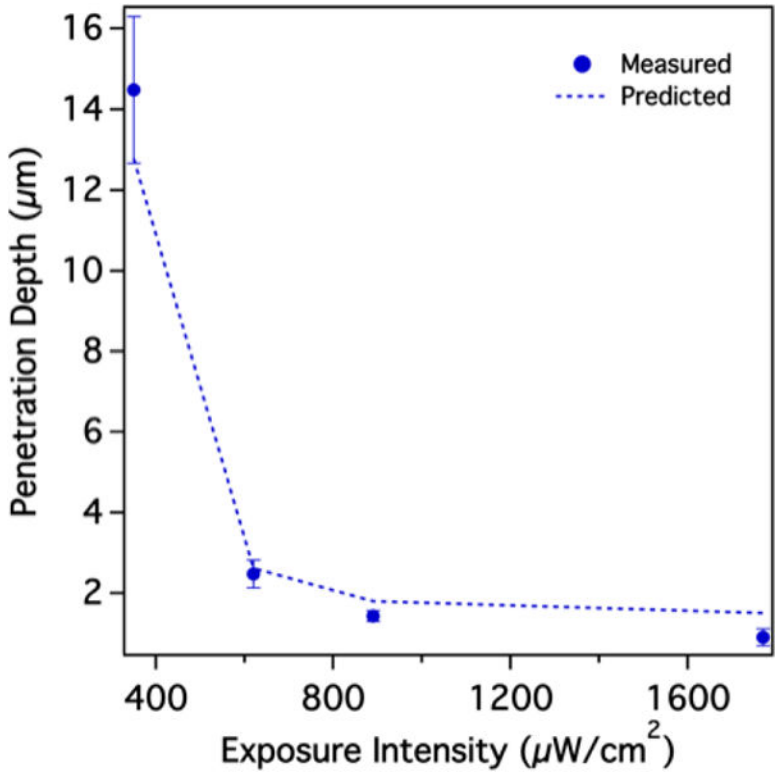

Figure 4.

Calculated NA penetration depth (dotted line), as determined by an extent of conversion threshold value of 38%, accurately predict empirical observations. (N = 30, error bars represent standard deviation)